Available online at www.sciencedirect.com

ScienceDirect

Procedia Engineering 64 (2013) 727 – 736

Procedia Engineering

www.elsevier.com/locate/procedia

International Conference On DESIGN AND MANUFACTURING, IConDM 2013

Comment [S1]: Elsevier to update w and page numbers.

Nonlinear dynamics of an Euler-Bernoulli beam with parametric and internal resonances

Bamadev Sahoo [a,*], L.N Panda[b], G.Pohit [c]

[a]Department of Mechanical Engineering, International Institute of Information Technology, Bhubaneswar,751003, India
[b]Department of Mechanical Engineering, College of Engineering and Technology, Bhubaneswar,751003, India
[c]Department of Mechanical Engineering, Jadavpur University, Kolkata,700032, India

Abstract

The nonlinear transverse vibration of a simply-supported travelling Euler-Bernoulli beam subjected to principal parametric resonance in presence of internal resonance is investigated. The variable velocity of beam is assumed to be comprised of a harmonically varying component superimposed over a mean value. The stretching of neutral axis introduces geometric cubic nonlinearity in the equation of motion of the beam. The natural frequency of second mode is approximately three times the natural frequency of first mode for a range of mean velocity of the beam, resulting in a three-to-one internal resonance. The method of multiple scales (MMS) is directly applied to the governing nonlinear integral-partial-differential equations and the associated boundary conditions. This results in a set of first order ordinary differential equations governing the modulation of amplitude and phase of the first two modes, which are analyzed numerically for principal parametric resonance of first mode. The nonlinear steady state response along with the stability and bifurcation of the beam are investigated. The dynamical behaviour of the system is observed in terms of periodic, quasiperiodic and chaotic responses, showing the influence of internal resonance.

Keywords: Three-to-one internal resonance; bifurcation; chaos; stability; perturbation technique.

* Corresponding author. Tel.: +91-674-3016025; fax: +91.674-3016009.
E-mail address: bamadev@iiit-bh.ac.in

doi:10.1016/j.proeng.2013.09.148

1. Introduction

The present work focuses on the nonlinear dynamic behaviour of travelling continua which cover many practical applications such as belts, conveyors, ropes, aerial cables, magnetic tapes and band saws. The situation of parametric resonances and internal resonances arising out of operating parameters can have profound influence on the dynamic behaviour of above applications which need to be suitably incorporated in their design features. Real-life axially moving systems rarely travel at a constant axial speed even when they are designed to be. Small imperfections caused by either geometrical or dynamical sources result in generation of an unsteady axial speed. This axial unsteady motion is modelled here by superimposing a harmonically fluctuating component over a mean travelling velocity. This harmonic fluctuation can cause parametric resonances hence it is important enough for investigation. The vast literature on axially moving continua vibration has been reviewed by Wickert and Mote [1] up to 1988. Oz et al. [2, 3] investigated principal and combination parametric resonances and stability analysis for an axially accelerating beam using the method of multiple scales. Riedel and Tan [4], Ozkaya et al. [5] and Bagdatli et al. [6] investigated non-linear transverse vibrations and internal resonances of travelling continua and plotted frequency response curves for different number of supports. Chin et al. [7] and Panda et al.[8-9] investigated principal parametric, combination parametric and internal resonances of hinged-clamped beams and pipe conveying pulsating fluid respectively. Recently a systematic research on travelling beam was pursued by Sze et al. [10] and Ghayesh et al. [11-13] involving nonlinear dynamic phenomenon of a variety of system models.

The present study is principal parametric resonance of first mode in which the influence of internal resonance is illustrated by the two mode equilibrium solutions of both amplitude and frequency response analysis. Besides the two mode solutions there is trivial mode solution. The system experiences pitchfork, Hopf and saddle node bifurcations with change in control parameters. The dynamic behaviour is depicted in terms of periodic, jump phenomena, quasiperiodic and chaotic responses.

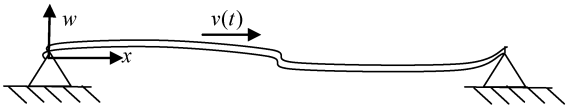

Fig. 1. Schematic diagram of an axially travelling simply supported beam with variable velocity.

2. Formulation of the problem

A uniform horizontal beam simply supported at both ends and travelling with a harmonically variable velocity (Fig.1) is considered. The beam is assumed to be an Euler-Bernoulli type in transverse vibration and nonlinearity is geometric in nature due to the mid-plane stretching effect. The non-dimensional equation of transverse motion of the beam including viscous damping [14] and viscoelastic damping [15] is given by

$$\ddot{w}+2v\dot{w}'+\dot{v}w'+(v^2-1)w''+v_f^2w''''+2\varepsilon\alpha\dot{w}''''+2\varepsilon\mu\dot{w}=\frac{1}{2}v_l^2w''\int_0^1 w'^2dx \tag{1}$$

The nondimensional scheme used here is

$$x=\frac{x^*}{L},\ t=t^*\sqrt{\frac{P}{\rho AL^2}},\ w=\frac{w^*}{L},\ v=\frac{v^*}{\sqrt{P/\rho A}},\ 2\varepsilon\alpha=\frac{E^*}{L^2}\left(\frac{I}{mE}\right)^{1/2},\ 2\varepsilon\mu=\frac{CL^2}{\sqrt{mEI}},\ v_l=\sqrt{\frac{EA}{P}},\ v_f=\sqrt{\frac{EI}{PL^2}}$$

where the variables with asterisk denote dimensional ones, dot and prime denote derivatives with respect to time and spatial variable x respectively. m is mass per unit length, ρ is density, A is cross sectional area, L is length, v_f is non dimensional flexural stiffness and v_l nondimensional longitudinal stiffness of beam. E^* is the coefficient of internal dissipation of the beam material (Kelvin-Voigt type). C is the external damping factor, α is nondimensional

material damping and μ is nondimensional viscous damping. Reordering the transverse displacement with the relation $w=\sqrt{\varepsilon}w^{\#}$, where $\varepsilon<1$, the system is converted into a weakly nonlinear one [3] and putting the variable velocity of beam, $v=v_0+\varepsilon v_1\sin\Omega t$, where v_0 is mean velocity, εv_1 is amplitude and Ω is the frequency of the harmonically varying component, Eq.(1) may be represented as (removing superscript "#")

$$\begin{aligned}&2\varepsilon\alpha\dot{w}''''+v_f^2w''''+\left[v_0^2+2\varepsilon v_0v_1\sin\Omega t-1\right]w''+\varepsilon v_1\Omega w'\cos\Omega t+2\left(v_0+\varepsilon v_1\sin\Omega t\right)\dot{w}'\\&+2\varepsilon\mu\dot{w}+\ddot{w}=\frac{1}{2}\varepsilon v_l^2w''\int_0^1w'^2dx\end{aligned}\tag{2}$$

With boundary conditions $w(0,\ t)=w(1,\ t)=w''(0,\ t)=w''(1,\ t)=0$ (3)

3. Method of analysis

An approximate solution to this weakly non-linear distributed parameter system in the form of a first order uniform expansion by using the direct perturbation technique of method of multiple scales (MMS) [5-9] is aimed. The time scale used here is $T_n=\varepsilon^n t,\ n=0,\ 1,\ 2,\ 3\ ...$ and the time derivatives are

$$\frac{d}{dt}=D_0+\varepsilon D_1+.....,\quad \frac{d^2}{dt^2}=D_0^2+2\varepsilon D_0D_1+.....,\quad D_n=\partial/\partial T_n,\quad n=0,1,2,3....\tag{4}$$

Assuming an expansion of the form $w(x,t,\varepsilon)=w_0(x,T_0,T_1)+\varepsilon w_1(x,T_0,T_1)+.....$ (5)

and equating coefficients of like powers of ε on both sides, we get

$$\begin{aligned}&O(\varepsilon^0):D_0^2w_0+2v_0D_0w_0'+(v_0^{\ 2}-1)w_0''+v_f^2w_0''''=0\\&w_0(0,\ t)=w_0(1,\ t)=w_0''(0,\ t)=w_0''(1,\ t)=0\end{aligned}\tag{6}$$

$$\begin{aligned}&O(\varepsilon^1):D_0^2w_1+2v_0D_0w_1'+v_f^2w_1''''+(v_0^{\ 2}-1)w_1''=-2v_0D_1w_0'-2v_1\sin\Omega tD_0\ w_0'-2D_0D_1w_0\\&-2\alpha D_0w_0''''-2\mu D_0w_0-2v_0v_1\sin\Omega t\ w_0''-v_1\Omega\cos\Omega t\ w_0'+\frac{1}{2}v_l^{\ 2}w_0''\int_0^1w_0'^2dx=0\\&w_1(0,\ t)=w_1(1,\ t)=w_1''(0,\ t)=w_1''(1,\ t)=0\end{aligned}\tag{7}$$

The solution of Eq. (6) may be written as $w_0(T_0,T_1,x)=\sum_{n=1}^{\infty}\phi_n(x)A_n(T_1)e^{i\omega_nT_0}+cc$ (8)

Where ϕ_n: mode shapes, ω_n: natural frequencies, and cc: complex conjugate. The mode shapes are [2]

$$\begin{aligned}\phi_n(x)=C_{1n}\Bigg\{&e^{i\beta_{1n}x}-\frac{\left(\beta_{4n}^2-\beta_{1n}^2\right)\left(e^{i\beta_{3n}}-e^{i\beta_{1n}}\right)}{\left(\beta_{4n}^2-\beta_{2n}^2\right)\left(e^{i\beta_{3n}}-e^{i\beta_{2n}}\right)}e^{i\beta_{2n}x}-\frac{\left(\beta_{4n}^2-\beta_{1n}^2\right)\left(e^{i\beta_{2n}}-e^{i\beta_{1n}}\right)}{\left(\beta_{4n}^2-\beta_{3n}^2\right)\left(e^{i\beta_{2n}}-e^{i\beta_{3n}}\right)}e^{i\beta_{3n}x}\\&+\left[-1+\frac{\left(\beta_{4n}^2-\beta_{1n}^2\right)\left(e^{i\beta_{3n}}-e^{i\beta_{1n}}\right)}{\left(\beta_{4n}^2-\beta_{2n}^2\right)\left(e^{i\beta_{3n}}-e^{i\beta_{2n}}\right)}+\frac{\left(\beta_{4n}^2-\beta_{1n}^2\right)\left(e^{i\beta_{2n}}-e^{i\beta_{1n}}\right)}{\left(\beta_{4n}^2-\beta_{3n}^2\right)\left(e^{i\beta_{2n}}-e^{i\beta_{3n}}\right)}\right]e^{i\beta_{4n}x}\Bigg\}\end{aligned}\tag{9}$$

where β_{in} are eigen values which satisfy the dispersive relation Eq.(10) and support condition Eq.(11) [2]

$$v_f^2\beta_{in}^4-\left(v_0^2-1\right)\beta_{in}^2-2v_0\omega_n\beta_{in}-\omega_n^2=0,\qquad i=1,2,3,4\tag{10}$$

$$\left(e^{i(\beta_{1n}+\beta_{2n})}+e^{i(\beta_{3n}+\beta_{4n})}\right)\left(\beta_{1n}^2-\beta_{2n}^2\right)\left(\beta_{3n}^2-\beta_{4n}^2\right)+\left(e^{i(\beta_{1n}+\beta_{3n})}+e^{i(\beta_{2n}+\beta_{4n})}\right)\left(\beta_{2n}^2-\beta_{4n}^2\right)$$
$$\left(\beta_{3n}^2-\beta_{1n}^2\right)+\left(e^{i(\beta_{2n}+\beta_{3n})}+e^{i(\beta_{1n}+\beta_{4n})}\right)\left(\beta_{1n}^2-\beta_{4n}^2\right)\left(\beta_{2n}^2-\beta_{3n}^2\right)=0 \tag{11}$$

Since the higher modes will decay with time due to the presence of damping and coriolis terms present in the equation, the first two modes will contribute to the long term system response. Hence, Eq. (8) is replaced by

$$w_0\left(T_0,T_1,x\right)=A_1\left(T_1\right)\phi_1\left(x\right)e^{i\omega_1T_0}+A_2\left(T_1\right)\phi_2\left(x\right)e^{i\omega_2T_0}+cc \tag{12}$$

The resonant frequency relations are $\omega_2=3\omega_1+\varepsilon\sigma_1$ and $\Omega=2\omega_1+\varepsilon\sigma_2$ (13)

Here σ_1 and σ_2 are detuning parameters. It is worthy to note, $\Omega=\omega_2-\omega_1+\varepsilon\left(\sigma_2-\sigma_1\right)$, a combination parametric resonance of the difference type is also activated simultaneously. Putting Eqs. (12-13), into Eq. (7), we get

$$D_0^2w_1+2v_0D_0w_1'+\left(v_0^2-1\right)w_1''+v_f^2w_1''''=\Gamma_1e^{i\omega_1T_0}+\Gamma_2e^{i(\omega_1T_0+\sigma_1T_1)}+\Gamma_3e^{i\omega_1T_0}+\Gamma_4e^{i(\omega_1T_0+\sigma_1T_1-\sigma_2T_1)}+\Gamma_5e^{i\omega_2T_0}$$
$$+\Gamma_6e^{i(\omega_2T_0-\sigma_1T_1)}+\Gamma_7e^{i(\omega_2T_0+\sigma_2T_1-\sigma_1T_1)}+cc+NST \tag{14}$$

where the terms Γ_n are defined in the Appendix. *NST* stands for terms that do not produce secular or small divisor terms. As the homogeneous part of Eq.(14) with its associated boundary conditions has a nontrivial solution, the corresponding nonhomogeneous problem has a solution only if a solvability condition is satisfied[7-9]. This requires the right hand side of Eq.(14) to be orthogonal to every solution of the adjoint homogeneous problem, which leads to the complex variable modulation equations for amplitude and phase,

$$2A_1'+8S_1A_1^2\bar{A}_1+8S_2A_1A_2\bar{A}_2+8g_1\bar{A}_1^2A_2e^{i\sigma_1T_1}+2\mu C_1A_1+2\alpha e_1A_1+2K_1\bar{A}_1e^{i\sigma_2T_1}+2K_2A_2e^{i(\sigma_1-\sigma_2)T_1}=0 \tag{15}$$

$$2A_2'+8S_4A_2^2\bar{A}_2+8S_3A_1A_2\bar{A}_1+8g_2A_1^3e^{-i\sigma_1T_1}+2\mu C_2A_2+2\alpha e_2A_2+2K_3A_1e^{i(\sigma_2-\sigma_1)T_1}=0 \tag{16}$$

where the prime denotes the differentiation with respect to slow time T_1 and S_i, g_i, K_i, C_i and e_i are defined in the Appendix. Over bar indicates complex conjugate. The terms in the above equations involving the internal frequency detuning parameter σ_1 are the contributions of the internal resonance in the system.

4. Stability and bifurcations

The evolutions of the equilibrium solutions, their stability and bifurcation analysis for principal parametric resonance are carried out from the modulation Eqs. (15-16) using

$$A_n=\frac{1}{2}\left[p_n\left(T_1\right)-iq_n\left(T_1\right)\right]e^{i\lambda_n(T_1)},n=1,2 \tag{17}$$

Putting this, in Eqs. (15-16), simplifying by trigonometric manipulations and separating the real and imaginary parts, we get the normalized reduced equations or the Cartesian form of modulation equations.

$$p_1'=-\vartheta_1q_1-\mu C_{1R}p_1-\mu C_{1I}q_1-\alpha e_{1R}p_1-\alpha e_{1I}q_1-g_{1R}\left(p_1^2p_2-p_2q_1^2+2p_1q_1q_2\right)+g_{1I}\left(2p_1q_1p_2-p_1^2q_2+q_1^2q_2\right)$$
$$-S_{1R}\left(p_1^3+p_1q_1^2\right)-S_{1I}\left(p_1^2q_1+q_1^3\right)-S_{2R}\left(p_1p_2^2+p_1q_2^2\right)-S_{2I}\left(q_1p_2^2+q_1q_2^2\right)-K_{1R}p_1+K_{1I}q_1-K_{2R}p_2-K_{2I}q_2 \tag{18}$$

$$q_1' = \vartheta_1 p_1 - \mu C_{1R} q_1 + \mu C_{1I} p_1 - \alpha e_{1R} q_1 + \alpha e_{1I} p_1 + g_{1R}\left(2p_1q_1p_2 - p_1^2q_2 + q_1^2q_2\right) + g_{1I}\left(2p_1q_1q_2 + p_1^2p_2 - p_2q_1^2\right)$$
$$+S_{1I}\left(p_1^3 + p_1q_1^2\right) - S_{1R}\left(p_1^2q_1 + q_1^3\right) - S_{2R}\left(q_1p_2^2 + q_1q_2^2\right) + S_{2I}\left(p_1p_2^2 + p_1q_2^2\right) + K_{1R}q_1 + K_{1I}p_1 - K_{2R}q_2 + K_{2I}p_2 \quad (19)$$

$$p_2' = -\vartheta_2 q_2 - \mu C_{2R} p_2 - \mu C_{2I} q_2 - \alpha e_{2R} p_2 - \alpha e_{2I} q_2 - g_{2R}\left(p_1^3 - 3p_1q_1^2\right) + g_{2I}\left(q_1^3 - 3p_1^2q_1\right)$$
$$-S_{4R}\left(p_2^3 + p_2q_2^2\right) - S_{4I}\left(q_2^3 + p_2^2q_2\right) - S_{3R}\left(p_1^2p_2 + p_2q_1^2\right) - S_{3I}\left(p_1^2q_2 + q_1^2q_2\right) - K_{3R}p_1 - K_{3I}q_1 \quad (20)$$

$$q_2' = -\vartheta_2 p_2 - \mu C_{2R} q_2 + \mu C_{2I} p_2 - \alpha e_{2R} q_2 + \alpha e_{2I} p_2 + g_{2R}\left(q_1^3 - 3p_1^2q_1\right) + g_{2I}\left(p_1^3 - 3p_1q_1^2\right)$$
$$-S_{4R}\left(q_2^3 + p_2^2q_2\right) + S_{4I}\left(p_2^3 + p_2q_2^2\right) - S_{3R}\left(p_1^2q_2 + q_1^2q_2\right) + S_{3I}\left(p_1^2p_2 + p_2q_1^2\right) - K_{3R}q_1 + K_{3I}p_1 \quad (21)$$

$$\text{Where } \vartheta_1 = 0.5\sigma_2 \text{ and } \vartheta_2 = 1.5\sigma_2 - \sigma_1 \quad (22)$$

Above equations are perturbed to evaluate the stability. The perturbed equation is

$$\left\{\Delta p_1' \;\; \Delta q_1' \;\; \Delta p_2' \;\; \Delta q_2'\right\}^{\mathrm{T}} = \left[J_c\right]\left\{\Delta p_1 \;\; \Delta q_1 \;\; \Delta p_2 \;\; \Delta q_2\right\}^{\mathrm{T}} \quad (23)$$

Where T denotes transpose and $\left[J_c\right]$ is the Jacobian matrix whose eigenvalues determine the stability and bifurcation of the system. The stability boundary for trivial state is obtained by setting $p_1 = q_1 = p_2 = q_2 = 0$. The nonlinear steady state response behaviour of the system is obtained from the normalized reduced Eqs. (18-21) by setting $p_1' = q_1' = p_2' = q_2' = 0$. These same set of equations are also used for the analysis of stability and bifurcation of trivial as well as nontrivial solutions. The analysis for dynamic solutions is carried out by numerically integrating the Eqs. (18-21) with different combinations of system parameters.

5. Results and discussion

The natural frequencies of the beam are numerically evaluated at different values of nondimensional mean velocity (v_0) with flexural stiffness $v_f = 0.2$ by simultaneous solution of dispersive relation (Eq. (10)) and support condition (Eq. (11)). For a value of $v_f = 0.2$, it is noticed that, at $v_0 = 0.513$, the natural frequency of second mode is approximately equal to three times that of the first mode, which implies the existence of 3:1 internal resonance. It is also noticed that, there are no other commensurable frequency relationships involving higher modes, so nonlinear interaction among higher modes is ruled out. The case of principal parametric resonance of first mode $(\Omega \approx 2\omega_1)$ in presence of internal resonance in the subcritical mean velocity regime of a travelling beam is analyzed. The trivial state stability boundary shown in Fig. 2 is plotted in terms of principal parametric frequency detuning (σ_2) and amplitude of fluctuating velocity component (v_1) for system parameters $v_f = 0.2, v_l = 40,\ v_0 = 0.7, \omega_1 = 2.7388, \omega_2 = 9.1403$ and for different material damping values. The book keeping parameter is taken as $\varepsilon = 0.01$ and the corresponding internal frequency detuning parameter is assumed to be $\sigma_1 = 92.39$. The region inside the boundary denotes instability.

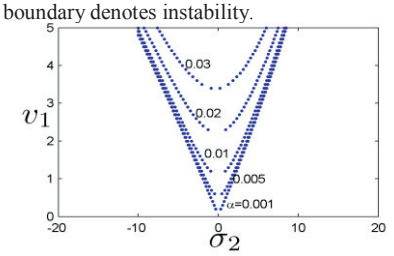

Fig. 2. Trivial state boundary for different damping parameters. Values of the nondimensional internal damping (α) indicated on the curves.

5.1. Stability and bifurcations of equilibrium solutions

Continuation algorithm is used to determine the nonlinear steady state response by solving the set of algebraic equations generated after setting $p_i' = q_i' = 0$ in the normalized reduced Eqs. (18-21). The stability and bifurcation of the equilibrium solutions are obtained from the eigen values of the Jacobean matrix at each point of the solution. The continuation algorithm used in the analysis is cross checked by plotting the frequency response and amplitude response curves of Chin et al. [7] and the results are found to be in good agreement as shown in Fig.3. Since the frequency and amplitude response curves are symmetrical about σ_2 and v_1 axes respectively, only positive sides of the response curves are shown.

Frequency response curves are obtained against variation in frequency detuning parameter σ_2 for first and second mode for $\mu = 0.05,\ \alpha = 0,\ v_1 = 10,\ v_l = 40, \sigma_1 = 92.39$ and are shown in Fig. 4. The normal continuous lines in the figure represent stable equilibrium solutions, the bold lines represent unstable foci, and the dotted lines denote saddles. The response curves exhibit a hardening-spring type of nonlinearity. With increase in σ_2 from a small value, the trivial stable solution loses stability at $\sigma_2 = -22.072$, through supercritical pitchfork bifurcation and results in a two mode non-trivial stable equilibrium solution. It is observed that the amplitude of the first mode increases initially then decreases, but the amplitude of second mode increases monotonically. When the value of σ_2 increases, the equilibrium solution becomes unstable at $H_1(\sigma_2 = 206.9504)$ through Hopf bifurcation and out of two pairs of complex conjugate eigenvalues, one pair crosses the imaginary axis from left half of the complex plane to right half. With further increase of σ_2, the same state continues until a saddle node bifurcation occurs at $SN(\sigma_2 = 301.9953)$ where the system response jumps to one of the two stable equilibrium branches, one trivial and other nontrivial, depending on the initial conditions as the solution converges to the closer equilibrium state as per the concept of region of attraction. With further increase in frequency detuning parameter, amplitude of the first mode increases monotonically along the nontrivial branch whereas the amplitude of second mode decreases continuously. Thus the amplitude of the indirectly excited second mode is limited to a fixed higher magnitude and for high values of σ_2, it becomes stagnant at fixed low amplitude while there is no such limitation for the directly excited first mode. When the detuning parameter decreases from a high value, the system follows either trivial or nontrivial stable equilibrium path, depending on the initial conditions. If the solution is nontrivial, with decrease of σ_2 value, the nontrivial stable branch loses stability via Hopf bifurcation at $H_2(\sigma_2 = 190.032)$ and regains stability via a reverse Hopf bifurcation at $H_3(\sigma_2 = 144.512)$. With further decrease in frequency detuning parameter, the nontrivial stable equilibrium branch merges with stable trivial equilibrium solution, the system loses and regains the stability at $H_6(\sigma_2 = 49.475)$ and $H_7(\sigma_2 = 44.607)$ respectively. At $\sigma_2 = 14.190$, the trivial equilibrium solution loses stability via subcritical/reverse pitchfork bifurcation and resulting in a jump of the response to the stable nontrivial branch of the solution. Again with further decrease of frequency detuning, the nontrivial stable solution branch loses stability through pitchfork bifurcation at $\sigma_2 = -22.071$, giving the way to trivial solution. The directly excited first mode dominates the indirectly excited second mode.

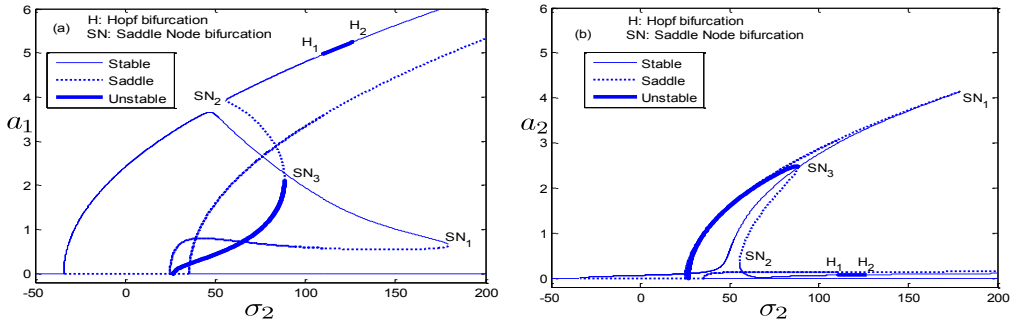

Fig. 3. Frequency response curves as obtained by continuation algorithm for the first and second modes when the first mode is parametrically excited for the system parameters Chin et al. [7].

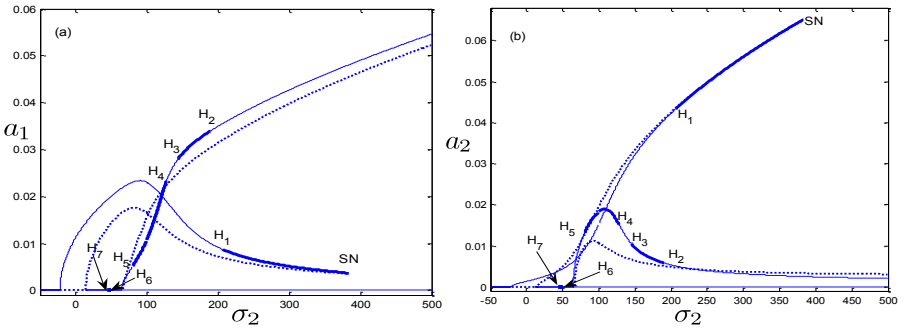

Fig.4. Frequency response curves for first mode (a) and second mode (b) for $\mu = 0.05$, $\alpha = 0$, $v_1 = 10$, v_l=40 and $\sigma_1 = 92.39$.

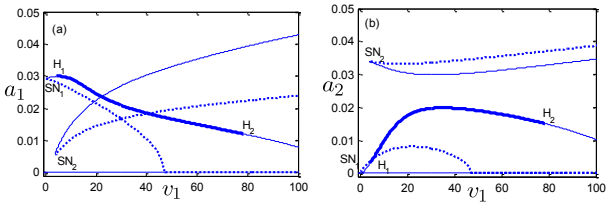

Fig.5. Amplitude response curves (a) first mode and (b) second mode for $\mu = 0.1$, $\alpha = 0$, v_l=40, $\sigma_1 = 92.39$ and $\sigma_2 = 150$.

Fig.5 represents the amplitude response plot for first two modes for system parameters $\mu = 0.1$, $\alpha = 0$, v_l=40, $\sigma_1 = 92.39$, $\sigma_2 = 150$, which may be illustrated in line of frequency response plots. It may be noted that like frequency response plots, amplitude response plots show Hopf and saddle node bifurcations but subcritical pitch fork bifurcation in place of super critical pitchfork bifurcation.

5.2. Dynamic solutions

Dynamic analysis of the system which is dependent on initial conditions is studied in the form of periodic, quasiperiodic and chaotic responses and some selected results are presented here. Figs. 6(a-d) show typical system response in terms of phase portraits (a, b) and time–traces (c, d) at $\sigma_2 = 382.9953$ corresponding to the lower nontrivial stable branch of the frequency response curve (Fig. 4) for $\mu = 0.05$, $\alpha = 0$, $v_1 = 10$, $\sigma_1 = 92.39$. The response is periodic about the nontrivial equilibrium solution when the time integration is started with the initial values $p_1 = 0.0018$, $q_1 = 0.0032$, $p_2 = -0.0459$ and $q_2 = -0.0462$. At another point along the same branch at $\sigma_2 = 370.2201$, the response is periodic in both modes for a long time then first mode jumps and shows a nontrivial periodic response while second mode jumps from a nontrivial to trivial periodic response as depicted through the time traces of Figs.7(c, d). Further along the same branch, typically at $\sigma_2 = 310.5201$, the system behaviour is quasiperiodic in both modes with a significant beating effect in second mode as shown in terms of the time trace in Fig.8(c). With further along the same branch at $\sigma_2 = 255.5201$, the response is quasiperiodic in both modes as illustrated by the characteristic closed form Poincare maps of the Figs. 9(c, d) and the two dimensional projections of the phase portraits onto the $p-q$ planes in Figs. 9(a, b). Typically at the parametric frequency detuning parameter $\sigma_2 = 117.4201$, the closed form Poincare maps for both modes get merged, which lead to chaotic behaviour of the system through quasiperiodic root. The uncountable number of points in the Poincare maps [Figs.10 (a, b)] and the time traces of both modes [Figs.10 (c, d)] depict the chaotic behaviour of the dynamic system. Hence the system experiences a wide range of dynamic responses with the change of system parameters.

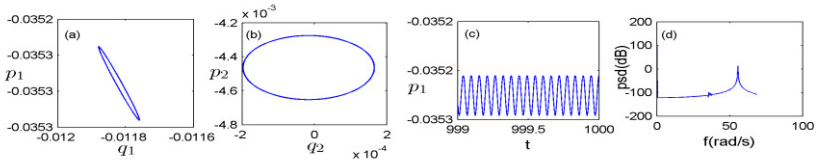

Fig. 6. Phase portraits (a, b) , time history(c) and FFT power spectra(d) in the lower nontrivial stable branch of the frequency response curve of Fig.4 for $\sigma_2 = 382.9953,\ \mu = 0.05,\ \nu_1 = 10,\ \alpha = 0,\ \sigma_1 = 92.39.$ \

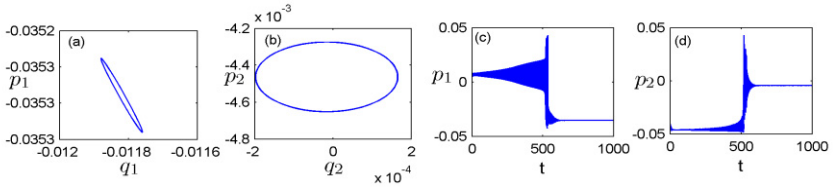

Fig. 7. Phase portraits (a, b) and time traces (c, d) in for $\sigma_2 = 370.2201,\ \mu = 0.05,\ \nu_1 = 10,\ \alpha = 0,\ \sigma_1 = 92.39.$

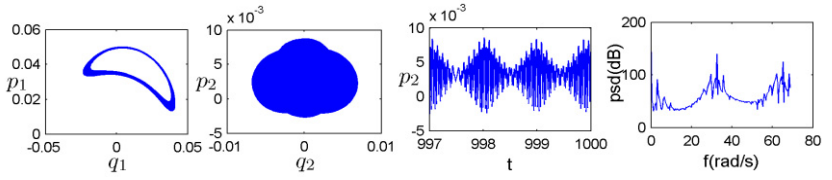

Fig. 8. Phase portraits (a, b) , time history(c) and FFT power spectra(d) for $\sigma_2 = 310.5201,\ \mu = 0.05,\ \nu_1 = 10,\ \alpha = 0,\ \sigma_1 = 92.39.$

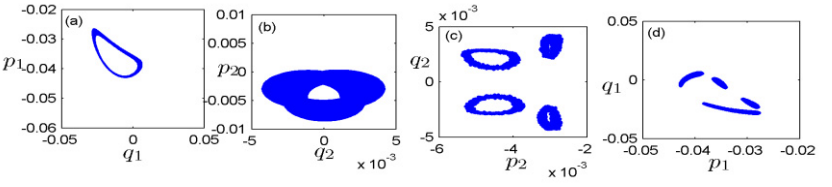

Fig. 9. Phase portraits (a, b) and Poincare maps(c, d) for $\sigma_2 = 255.5201,\ \mu = 0.05,\ \nu_1 = 10,\ \alpha = 0,\ \sigma_1 = 92.39.$

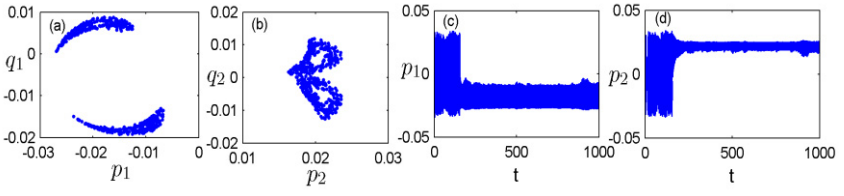

Fig. 10. Poincare maps (a, b) and time traces(c, d) for $\sigma_2 = 117.4201,\ \mu = 0.05,\ \nu_1 = 10,\ \alpha = 0,\ \sigma_1 = 92.39.$

6. Conclusions

Nonlinear transverse dynamics of an axially travelling beam in presence of internal resonance is investigated by using the method of multiple scales (MMS) for the case of principal parametric resonance of first mode. The influence of internal resonance on the system behaviour is numerically evaluated in steady state and dynamic solutions. Stability boundaries of trivial state are obtained for different values of internal dissipation. The stability and bifurcations of equilibrium solutions are analyzed in the form of frequency-response and amplitude response plots. Due to modal interaction, the system exhibits response only in directly excited first mode and indirectly excited second mode, where as other modes die down due to damping effect. It has been shown in frequency response plot that the non-trivial steady state solutions bifurcate from trivial solutions through supercritical pitchfork bifurcations. There is upper bound in the system response in the indirectly excited second mode but no such upper bound exists for the directly excited first mode. Besides the pitchfork bifurcations, the system experiences Hopf and saddle-node bifurcations.

The dynamic solutions in the form of periodic, quasi-periodic and chaotic are captured with the help of time history, two dimensional phase portraits, Poincare maps, and FFT power spectra plots. Also, the system exhibits jump phenomena and due to variations of control parameters, its behaviour changes to chaotic response through quasiperiodic route. The system exhibits a wide array of dynamic responses with variation of control parameters.

Appendix

$$\Gamma_1 = -2i\omega_1 A_1'\phi_1 - 2v_0 A_1'\phi_1' - 2i\mu\omega_1 A_1\phi_1 - 2i\alpha\omega_1 A_1\phi_1'' + \frac{1}{2}v_l^2\left\{2A_1^2\bar{A}_1\phi_1''\int_0^1\phi_1'\bar{\phi}_1'dx + A_1^2\bar{A}_1\bar{\phi}_1''\int_0^1\phi_1^2dx + 2A_1A_2\bar{A}_2\bar{\phi}_2''\int_0^1\phi_1'\phi_2'dx\right.$$

$$\left. + 2A_1A_2\bar{A}_2\phi_1''\int_0^1\phi_2'\bar{\phi}_2'dx + 2A_1A_2\bar{A}_2\phi_2''\int_0^1\phi_1'\bar{\phi}_2'dx\right\}\ \Gamma_2 = \frac{1}{2}v_l^2\left\{2\bar{A}_1^2A_2\bar{\phi}_1''\int_0^1\phi_2'\bar{\phi}_1'dx + \bar{A}_1^2A_2\phi_2''\int_0^1\bar{\phi}_1^2\,dx\right\};$$

$$\Gamma_3 = \bar{A}_1\left\{v_1\omega_1\bar{\phi}_1' - \frac{v_1\Omega}{2}\bar{\phi}_1' + iv_0v_1\bar{\phi}_1''\right\};\ \Gamma_4 = A_2\left\{v_1\omega_2\phi_2' - \frac{v_1\Omega}{2}\phi_2' - iv_0v_1\phi_2''\right\}$$

$$\Gamma_5 = -2i\omega_2A_2'\phi_2 - 2v_0A_2'\phi_2' - 2\mu i\omega_2A_2\phi_2 - 2\alpha i\omega_2A_2\phi_2'' + \frac{1}{2}v_l^2\left\{A_2^2\bar{A}_2\bar{\phi}_2''\int_0^1\phi_2'^2\,dx + 2A_1\bar{A}_1A_2\phi_2''\int_0^1\phi_1'\,\bar{\phi}_1'dx + 2A_1\bar{A}_1A_2\bar{\phi}_1'\int_0^1\phi_1'\phi_2'dx\right.$$

$$\left. + 2A_2^2\bar{A}_2\bar{\phi}_2''\int_0^1\phi_2'\bar{\phi}_2'dx + 2A_1\bar{A}_1A_2\phi_1''\int_0^1\phi_2'\bar{\phi}_1'dx\right\};\ \Gamma_6 = \frac{1}{2}v_l^2\left\{A_1^3\phi_1''\int_0^1\phi_1'^2dx\right\};\ \Gamma_7 = A_1\left\{-v_1\omega_1\phi_1' - \frac{v_1\Omega}{2}\phi_1' + iv_0v_1\phi_1''\right\};$$

$$S_1 = \frac{\frac{1}{16}v_l^2\left\{2\int_0^1\phi_1''\bar{\phi}_1dx\int_0^1\phi_1'\bar{\phi}_1'dx + \int_0^1\bar{\phi}_1''\bar{\phi}_1dx\int_0^1\phi_1'^2dx\right\}}{-\left\{i\omega_1\int_0^1\phi_1\bar{\phi}_1dx + v_0\int_0^1\phi_1'\bar{\phi}_1dx\right\}};\ S_2 = \frac{\frac{1}{8}v_l^2\left\{\int_0^1\bar{\phi}_2''\bar{\phi}_1dx\int_0^1\phi_1'\phi_2'dx + \int_0^1\phi_1''\bar{\phi}_1dx\int_0^1\phi_2'\bar{\phi}_2'dx + \int_0^1\phi_2''\bar{\phi}_1dx\int_0^1\phi_1'\bar{\phi}_2'dx\right\}}{-\left\{i\omega_1\int_0^1\phi_1\bar{\phi}_1dx + v_0\int_0^1\phi_1'\bar{\phi}_1dx\right\}};$$

$$S_3 = \frac{\frac{1}{8}v_l^2\left\{\int_0^1\phi_2''\bar{\phi}_2dx\int_0^1\phi_1'\bar{\phi}_1dx + \int_0^1\bar{\phi}_1''\bar{\phi}_2dx\int_0^1\phi_1'\phi_2'dx + \int_0^1\phi_1''\bar{\phi}_2dx\int_0^1\phi_2'\bar{\phi}_2'dx\right\}}{-\left\{i\omega_2\int_0^1\phi_2\bar{\phi}_2dx + v_0\int_0^1\phi_2'\bar{\phi}_2dx\right\}};\ S_4 = \frac{\frac{1}{16}v_l^2\left\{2\int_0^1\phi_2''\bar{\phi}_2dx\int_0^1\phi_2'\bar{\phi}_2'dx + \int_0^1\bar{\phi}_2''\bar{\phi}_2dx\int_0^1\phi_2'^2dx\right\}}{-\left\{i\omega_2\int_0^1\phi_2\bar{\phi}_2dx + v_0\int_0^1\phi_2'\bar{\phi}_2dx\right\}};$$

$$C_1=\frac{-i\omega_1\int_0^1\phi_1\bar{\phi}_1dx}{-\left\{i\omega_1\int_0^1\phi_1\bar{\phi}_1dx+v_0\int_0^1\phi_1'\bar{\phi}_1dx\right\}};\ C_2=\frac{-i\omega_2\int_0^1\phi_2\bar{\phi}_2dx}{-\left\{i\omega_2\int_0^1\phi_2\bar{\phi}_2dx+v_0\int_0^1\phi_2'\bar{\phi}_2dx\right\}};\ e_1=\frac{-i\omega_1\int_0^1\phi_1''''\bar{\phi}_1dx}{-\left\{i\omega_1\int_0^1\phi_1\bar{\phi}_1dx+v_0\int_0^1\phi_1'\bar{\phi}_1dx\right\}};$$

$$e_2=\frac{-i\omega_2\int_0^1\phi_2''''\bar{\phi}_2dx}{-\left\{i\omega_2\int_0^1\phi_2\bar{\phi}_2dx+v_0\int_0^1\phi_2'\bar{\phi}_2dx\right\}};\ g_1=\frac{\frac{1}{16}v_l^2\left\{2\int_0^1\bar{\phi}_1''\bar{\phi}_1dx\int_0^1\phi_2'\bar{\phi}_1'dx+\int_0^1\phi_2''\bar{\phi}_1dx\int_0^1\bar{\phi}_1^2dx\right\}}{-\left\{i\omega_1\int_0^1\phi_1\bar{\phi}_1dx+v_0\int_0^1\phi_1'\bar{\phi}_1dx\right\}};\ g_2=\frac{\frac{1}{16}v_l^2\left\{\int_0^1\phi_1''\bar{\phi}_2dx\int_0^1\phi_1^2dx\right\}}{-\left\{i\omega_2\int_0^1\phi_2\bar{\phi}_2dx+v_0\int_0^1\phi_2'\bar{\phi}_2dx\right\}};$$

$$K_1=\frac{\frac{1}{2}\left\{v_1\omega_1\int_0^1\bar{\phi}_1'\bar{\phi}_1dx-\frac{v_1\Omega}{2}\int_0^1\bar{\phi}_1'\bar{\phi}_1\,dx+iv_0v_1\int_0^1\bar{\phi}_1''\bar{\phi}_1\,dx\right\}}{-\left\{i\omega_1\int_0^1\phi_1\bar{\phi}_1dx+v_0\int_0^1\phi_1'\bar{\phi}_1dx\right\}};\ K_2=\frac{\frac{1}{2}\left\{v_1\omega_2\int_0^1\phi_2'\bar{\phi}_1dx-\frac{v_1\Omega}{2}\int_0^1\phi_2'\bar{\phi}_1\,dx-iv_0v_1\int_0^1\phi_2''\bar{\phi}_1\,dx\right\}}{-\left\{i\omega_1\int_0^1\phi_1\bar{\phi}_1dx+v_0\int_0^1\phi_1'\bar{\phi}_1dx\right\}};$$

$$K_3=\frac{\frac{1}{2}\left\{-v_1\omega_2\int_0^1\phi_1'\bar{\phi}_2dx-\frac{v_1\Omega}{2}\int_0^1\phi_1'\bar{\phi}\,dx+iv_0v_1\int_0^1\phi_1''\bar{\phi}_2\,dx\right\}}{-\left\{i\omega_2\int_0^1\phi_2\bar{\phi}_2dx+v_0\int_0^1\phi_2'\bar{\phi}_2dx\right\}};$$

References

[1] Wickert, J.A., Mote Jr., C.D., 1988, Current research on the vibration and stability of axially moving materials, Shock and Vibration Digest 20, pp. 3-13.

[2] Oz, H.R., Pakdemirli, M., 1999, Vibrations of an axially moving beam with time-dependent velocity, Journal of Sound and Vibration 227(2), pp. 239-257.

[3] Oz, H.R., Pakdemirli, M., Boyaci, H., 2001, Non-linear Vibrations of an axially moving beam with time-dependent velocity, International Journal of Non-linear Mechanics 36, 227(2), pp. 107-115.

[4] Riedel, C.H., Tan, C.A., 2002, Coupled, forced response of an axially moving strip with internal resonance, International Journal of Nonlinear Mechanics 37, pp. 101-116.

[5] Ozkaya, E., Bagdatli, S.M., Oz, H.R., 2008, Nonlinear transverse vibrations and 3:1 internal resonances of a beam with multiple supports, Journal of Vibration and Acoustics 130(2), pp.1-11.

[6] Bagdatli, S.M., Oz, H.R., Ozkaya, E., 2011, Nonlinear transverse vibrations and 3:1 internal resonances of a tensioned beam on multiple supports, Mathematical and Computational Applications 16(1), pp. 203-215.

[7] Chin, C.M., Nayfeh, A.H., 1999, Three-to-one internal resonance in parametrically excited Hinged-clamped beams, Nonlinear Dynamics 20, pp. 131-158.

[8] Panda, L.N., Kar, R.C., 2007, Nonlinear dynamics of a pipe conveying pulsating fluid with parametric and internal resonances, Nonlinear Dynamics 49, pp. 9-30.

[9] Panda, L.N., Kar, R.C., 2008, Nonlinear dynamics of a pipe conveying pulsating fluid with combination, principal parametric and internal resonances, Journal of Sound and Vibration 309, pp. 375-406.

[10] Sze, K.Y., Chen, S.H., Huang, J.L., 2005, The incremental harmonic balance method for nonlinear vibration of axially moving beams, Journal of Sound and Vibration 281, pp. 611-626.

[11] Ghayesh, M.H., 2011, Nonlinear forced dynamics of an axially moving viscoelastic beam with an internal resonance, International Journal of Mechanical Sciences 53, pp. 1022-1037.

[12] Ghayesh, M.H., 2012, Subharmonic dynamics of an axially accelerating beam, Archive of Applied Mechanics 82, pp.1169-1181.

[13] Ghayesh, M.H., Amabili, M., 2013, Steady-state transverse response of an axially moving beam with time-dependent axial speed, International Journal of Non-Linear Mechanics 49, pp. 40-49.

[14] Chakraborty, G., Mallick, A.K., 1999, Stability of an accelerating beam, Journal of Sound and Vibration 27(2), pp. 309-320.

[15] Paidoussis, M.P.,1975, Flutter of conservative systems of pipe conveying incompressible fluid, Journal of Mechanical Engineering and Science 17(1), pp.19-25.

[16] Pakdemirli, M., Boyaci, H., 1985, Comparison of direct perturbation methods with discretization-perturbation methods for nonlinear vibrations. Journal of Sound and Vibration 186, pp. 837-845.